Modeling the thickness of perennial ice covers on stratified lakes of the Taylor Valley, Antarctica

M. K. Obryk[1,2], P. T. Doran[2], J. A. Hicks[3], C. P. McKay[4], J. C. Priscu[5]

[1]Departemnt of Geology, Portland State University, Portland, Oregon, USA
[2]Department of Geology and Geophysics, Louisiana State University, Baton Rouge, Louisiana, USA
[3]Engineering Sciences and Applied Mathematics, Northwestern University, Evanston, Illinois, USA
[4]Space Science Division, NASA Ames Research Center, Moffett Field, California, USA
[5]Department of Land Resources and Environmental Sciences, Montana State University, Bozeman, Montana, USA

Abstract

A ~~one-dimensional~~ ice cover model was developed to predict and constrain drivers of long-term ice thickness trends in chemically stratified lakes of Taylor Valley, Antarctica. The model is driven by surface radiative heat fluxes and heat fluxes from the underlying water column. The model successfully reproduced 16 ~~years~~ (between 1996 and 2012) of ice thickness changes for west lobe of Lake Bonney (average ice thickness = 3.53 m; RMSE = 0.09 m, n = 118) and Lake Fryxell (average ice thickness = 4.22 m; RMSE = 0.21 m, n = 128). Long-term ice thickness trends require coupling with the thermal structure of the water column. The heat stored within the temperature maximum of lakes exceeding a liquid water column depth of 20 m can either impede or facilitate ice thickness change depending on the predominant climatic trend (~~temperature~~ cooling or warming). As such, shallow (< 20 m deep water columns) perennially ice-covered lakes without deep temperature maxima are more sensitive indicators of climate change. The long-term ice thickness trends are a result of surface energy flux and heat flux from the deep temperature maximum in the water column, the latter of which results from absorbed solar radiation.

Introduction

Perennially ice-covered lakes in the McMurdo Dry Valleys, Antarctica have long been studied as novel habitats for life. Ice covers offer protection from wind-driven turbulence, and together with strong salinity gradients within the lakes, permit permanent vertical temperature stratification, the development of supersaturated gas concentrations (Priscu and others, 1996; Andersen and others, 1998; Wharton and others, 1986), and altered sediment pathways (Doran and others, 1994). Although the permanent ice covers provide insulation from the atmosphere, they do allow penetration of solar radiation, often producing thermal maxima deep in the water column in association with saltier water (Vincent and others, 2008). Despite the deep temperature maxima, the salt gradient maintains vertically stable water columns (Spigel & Priscu, 1996). Ice cover thickness is balanced primarily by ablation at the surface and ice growth at the bottom (Chinn, 1993; Adams and others, 1998). McKay and others (1985) developed a steady state energy-balance model that predicts ice cover thickness based on surface ablation (mass loss by all means) rates and latent heat of ice formation. Latent heat release, associated with ice growth, is conducted upwards and lost to the atmosphere due to ablation (McKay and others, 1985). Because of the tight coupling of lake ice thickness to atmospheric processes, the ice covers should respond directly to changing climate (Launiainen & Cheng, 1998; Reid & Crout, 2008; Wharton and others, 1992).

Lakes in Taylor Valley, one of the McMurdo Dry Valleys have been perennially ice-covered since at least 1903, when they were discovered by Robert Falcon Scott (Scott, 1905). Taylor Valley lake volumes are controlled by a balance of summer temperatures ~~warm~~ enough to generate melt from local glaciers, yet ~~cold~~ enough for the lake ice covers to persist through the summer (Chinn, 1993). The ice thickness in Taylor Valley lakes has been fluctuating between 3 and 6 m over the past two decades (McKay and others, 1985; Doran and others, 2002b). Ice thickness of Lake Hoare (freshwater lake) in McMurdo Dry Valleys thinned from 1977 to 1986 at a rate of >0.28 m a^{-1} (Wharton and others, 1989); however little climate data ~~is~~ available for this time period. Between 1986 and 1999, ~~its~~ lake-ice thickness increased at a rate of 0.11 m a^{-1} in association with an annual air temperature decrease of 0.7~~°C per decade~~ (Doran and others, 2002b). This period of pronounced cooling was terminated by one of the warmest summers on record, resulting in a significant lake level rise (Doran and others, 2008; Barrett and others, 2008). Following this warm pulse, lake-ice thicknesses have been decreasing since early- to mid-2000 at rates between 0.07 and 0.18 m a^{-1} (unpublished data). Here we present results from a lake ice model that allowed us to differentiate between the influence of atmospheric processes (i.e., changes in climate) and the long-term heat storage in the water column on lake ice thickness.

Site Description

The McMurdo Dry Valleys, East Antarctica ~~is~~ an ice-free region with perennially ice-covered lakes typically located in hydrologically closed-basins. This arid environment ~~is a result of~~ combination of low precipitation and the Transantarctic Mountains blocking the ice sheet flow (Chinn, 1993). The mean annual valley-bottom temperatures range from -14.8 °C to -30.0 °C, with summer temperatures high enough to enable glacial melt, which feeds into the lakes (Doran and others, 2002a). The two lakes in this study, west lobe of Lake Bonney (WLB) and Lake Fryxell (Figure 1), are in different microclimatic zones in Taylor Valley. WLB is located ~~approximately~~ 27 km from the coast and influenced by strong, dry winds from the Antarctic

plateau, whereas Lake Fryxell, adjacent to the coast, is influenced by moist coastal winds (Fountain and others, 1999; Doran and others, 2002a). Lake levels in Taylor Valley have been rapidly increasing since early 2000's and the depths of WLB and Lake Fryxell, as of Jan 2012 are 41.2 and 22.4 m deep, respectively (data obtained from www.mcmlter.org). The average ice thickness between 1996 and 2012 of WLB and Lake Fryxell is 3.5 and 4.2 m, respectively.

Model Development

General Model Description

Launiainen and Cheng (1998) provide a general description and evolution of different ice models since thermodynamic modeling of ice began in the late 1800's. Despite extensive research, no universal lake ice model is available, as each lake has different characteristics and unique adjustments are necessary (Reid & Crout, 2008). The model we developed uses generalized parameters to make it adaptable to other stratified perennially ice-covered lakes.

The model developed here is modified from an approach by Launiainen and Cheng (1998) and Reid and Crout (2008). The model considers 1) the dynamic coupling of atmospheric processes with ice (surface energy balance), 2) the dynamic coupling of the water column with ice (moving boundary condition), and 3) heat conduction within the ice and the water column (two one-dimensional heat equations) (Figure 2). Three boundaries are defined in the model: atmosphere/ice, ice/water, and water/bedrock. The vertical temperature profile of the ice and the water column is solved using a spectral method based on the state of the boundaries. The main advantage of the spectral method over the finite difference or the finite element method is a higher degree of accuracy for smooth problems allowing a coarse computational grid (Trefethen, 2000).

Surface ice temperature was calculated based on the summation of surface radiative fluxes and becomes the top boundary condition for the one-dimensional heat equation (see *Surface Energy Balance* section for details). Known surface ice temperature allows for the calculation of temperature profiles of the ice as the temperature at the bottom of the ice is set to the freezing point. The water temperature profile is solved using a second one-dimensional heat equation, with penetrating solar radiation acting as the heat flux contribution to the water column (water/bedrock boundary temperature is fixed). Ice and water temperature profiles are coupled at the ice/water interface accounting for the conductive, latent, and sensible heat fluxes. The ice/water interface is a moving Dirichlet boundary condition, which forces the solution of a heat equation to converge at the freezing point of the water. This boundary incorporates latent heat fluxes associated with the phase transition (Gupta, 2003).

A one-dimensional solution to the heat equation is valid because it succinctly approximates the physical processes. The lateral thermal gradient can be considered negligible with regards to depth, allowing a one-dimensional heat equation to be employed because vertical exchanges are much greater than lateral exchanges. Heat exchange within the ice is assumed to occur through conduction (even though this assumption can break down when ice is isothermal) and is based on a temperature gradient defined at the atmosphere/ice and ice/water boundaries. The heat within the ice diffuses vertically at a rate defined by the thermal diffusivity of the ice and the temperature gradient. Similar to the approach used for the ice, a one-dimensional heat equation is used to calculate the temperature profile of the water column in order to better constrain heat fluxes at the ice/water boundary. The water column of Taylor Valley lakes we modeled are chemically stratified and vertical diffusive heat transfer occurs at the molecular level; our study lakes have no vertical convective mixing (Spigel & Priscu, 1998). Horizontal motion in the lakes

can occur as the result of horizontal advection caused by lateral stirring induced by contact with glacial ice (WLB) and stream input during the austral summer (Spigel ~~&~~ Priscu, 1998) and are not considered in this model.

The model employs dimensional analysis permitting the grouping of variables that describe physical parameters in a dimensionless form. Dimensional analysis is based on the Buckingham π-theorem, allowing for the reduction of independent variables by k dimensions, where k represents physical dimensions required to describe n variables used in the model. Then, it follows that there will be π dimensionless groups based on $n - k$. As a result, this method reduces the complexity of the model and, consequently, reduces the complexity of the solution to the heat equation and allows the computational domain to be fixed at [-1, 1], regardless of the ice thickness.

Model input data

Meteorological data used in the model include air temperature, shortwave radiation (400 to 1100 nm), relative humidity~~,~~ and wind speed. Longwave upwelling and downwelling radiation, and turbulent sensible and latent heat fluxes were parameterized using equations adapted from Reid and Crout (2008), discussed in more detail below. The albedo of the ice was simulated as a spline function based on a ~~five-~~month data record (September to February) from WLB, obtained from Fritsen and Priscu (1999). Based on this record, the largest albedo change (increase) occurs during the summer months when ice morphology and hoar frost in air bubbles change due to the thermal properties of the ice (Fritsen ~~&~~ Priscu, 1999~~;~~ Adams and others, 1998). The missing albedo data for the remainder of the year (spring and fall) were extrapolated. Any error in this assumption is reduced by the diminished importance of radiation during these periods and the complete lack of radiation during the winter months.

The model was run with 16 ~~years~~ of meteorological data obtained from Lake Bonney's meteorological weather station, located on the southern shore of east lobe of Lake Bonney (Fig~~ure~~ 1). Data were collected using Campbell Scientific dataloggers (CR10 and 21X) at 30 s sampling intervals and stored as 15 min averages (Doran and others, 1995~~;~~ Doran and others, 2002a). Air temperature was measured using Campbell 207 and 107 temperature probes at a 3 m height (Doran and others, 1995). Shortwave radiation was obtained with Li-Cor LI200S and LI200X silicon pyranometer (Doran and others, 1995). Wind speed was obtained with R.~~-~~M. Young model 05103 wind monitors (Doran and others, 1995). The model was run at ~~12-hour~~ intervals, dynamically averaging high-resolution data (15 min intervals) during simulations.

Gaps in data occurred, ranging from hours to months, due to either failed sensors or failed dataloggers. Missing shortwave radiation was remedied by using well-known published equations (~~see~~ *Shortwave Radiation* section) dynamically substituting gaps in data during model simulations. Missing air temperature values were substituted by using a function based on daily averaged temperatures from 16 ~~years~~ of data. Missing relative humidity and wind speed data represent cumulative 6.6 and 4.6 % of the entire dataset~~,~~ respectively, and were determined by a uniform random number generator (within the upper and lower limit of each variable). Uniform distribution ensures that a value within the set range has equal probability of being generated.

Validation data

Ice thickness data were measured manually at the drill hole sites from the bottom of the ice to the piezometric water level, representing the ice thickness ~~in water equivalents~~. Due to logistical constraints, the ice thickness data were only available during the austral summers when the ice

was most dynamic, with the exception of an extended season in 2008, when data were obtained through late ~~fall~~ (into March). Replicate ice thickness measurements (3 to 10) were made during the same day (within a 10 m^2 grid) or within ~~two days~~ of each other, and show a large variability (largest standard deviation of seasonally measured ice thickness is 0.54), introducing error during the validation procedure of the model.

Continuous ablation data were measured from suspended pressure transducers at the bottom of the ice (Dugan and others, 2013). Data were recorded at ~~one minute~~ intervals (averaged over 20 min), using Druck PDCR 1830 or Keller Series 173 pressure transducers and stored on Campbell Scientific CR10X and CR1000 dataloggers (Dugan and others, 2013).

Surface Energy Balance

The vertical temperature profile of the ice and its evolution over time can be modeled utilizing a ~~one-dimensional~~ unsteady heat equation:

$$pc\frac{\partial T(z,t)}{\partial t} = -\frac{\partial}{\partial z}\left(-k\frac{\partial T(z,t)}{\partial z} + I(z,t)\right) \quad (1)$$

where p is the density of ice or water, c is the specific heat capacity of ice or water, T is temperature, z is depth, t is time, k is thermal conductivity~~,~~ and I is the heat source term within the ice and the water column. All constants and variables are summarized in Appendix A. Shortwave radiation is the only significant flux that contributes to the I term because ice is opaque in infrared and transparent in the visible spectrum (McKay and others, 1994). The transmittance of sunlight through the perennially ice-covered lakes in Taylor Valley can be approximated using the Lambert-Beer law (McKay and others, 1985), by defining a constant extinction coefficient. However, this technique does not account for the absorbed near-infrared radiation at the very surface of the ice (Bintanja ~~&~~ Vandenbroeke, 1995~~;~~ Brandt ~~&~~ Warren, 1993). A method used in Bintanja and Vandenbroeke (1995) was adapted that parameterized solar energy by partitioning absorbed solar energy at the very surface and subsurface of the ice, expressing the heat source term as:

$$I(z,t) = (1-\chi)(1-\alpha)Q_s e^{-\kappa z} \quad (2)$$

where χ accounts for a fraction of absorbed shortwave radiation at the surface, α is albedo, Q_s is shortwave radiation, and κ is the extinction coefficient of the ice at depth z.

The top boundary condition for ~~Eq.~~ (1) is calculated based on the summation of all surface radiative heat fluxes:

$$F(T_s) = \chi(1-\alpha)Q_s + Q_b + Q_d + Q_h + Q_l + F_i \quad (3)$$

where T_s is ice surface temperature, Q_s is shortwave radiation, Q_b is longwave upwelling radiation, Q_d is longwave downwelling radiation, Q_h is sensible heat flux, Q_l is latent heat flux, and F_i is the heat conduction at the ice surface. However, T_s cannot be solved based on this equation alone because the longwave upwelling radiation, sensible~~,~~ and conductive heat fluxes depend on the surface ice temperature. The Newtonian iterative method is implemented in the model to solve for T_s, which is used to determine the temperature gradient within the ice cover. Positive fluxes are toward the ice, negative are away from the ice.

Shortwave Radiation

Shortwave radiation (Q_s) for an atmosphere-less Earth is defined as:

$$Q_s = ScosZ \tag{4}$$

where S is a solar constant and Z is a solar zenith, derived using solar declination, solar angle, and latitude. Atmospheric attenuation of Q_s requires modification of Eq. (4) with empirical parameters related to the study site and numerous equations are available in the literature (Lumb, 1964; Bennett, 1982; Reid & Crout, 2008). Parameterization of Q_s for an Antarctic site has been done by Reid and Crout (2008) and was adopted here.

Longwave Radiation

Longwave upwelling radiation (Q_b) was modeled based on the Stefan-Boltzmann law as a function of surface ice temperature and is expressed as:

$$Q_b = -\varepsilon_i \sigma_s T_s^4 \tag{5}$$

where ε_i represents dimensionless surface emissivity and σ_s is the Stefan-Boltzmann constant (Launiainen & Cheng, 1998).

Downwelling longwave radiation (Q_d) takes a form of Eq. (5) but is controlled by surface air temperature (T_a) and cloud cover (C) (Guest, 1998; Konig-Langlo & Augstein, 1994). Cloud cover is expressed as a unitless value (from 0 to 1) representing the fraction of sky covered by clouds. However, cloud cover data for the WLB is unavailable. Missing cloud cover data can be treated as an adjustable parameter in models driven by surface energy balance (Liston and others, 1999). Here, we chose C to be generated by a random number generator (uniform distribution) at daily intervals in order to simplify the model by decreasing the number of adjustable parameters. Downwelling longwave radiation requires parameterization of atmospheric emissivity (ε_a), which accounts for C, vapor distribution, and temperature (Konig-Langlo & Augstein, 1994). The equation for Q_d was adopted from Konig-Langlo and Augstein (1994) because they parameterized ε_a based on Antarctic datasets, which is applicable for high-latitudes:

$$Q_d = (0.765 + 0.22C^3)\sigma_s T_a^4 \tag{6}$$

Sensible and Latent Heat Flux at the Ice Surface

Turbulent sensible (Q_h) and latent ~~heat~~ (Q_l) fluxes at the atmosphere/ice boundary are modeled after Launiainen and Cheng (1998) and are expressed as:

$$Q_h = \rho_a c_a C_H (\Delta T) V \tag{7}$$

$$Q_l = \rho_a R_l C_E (\Delta q) V \tag{8}$$

where ρ_a is air density, c_a is specific heat capacity of air, V is wind speed, R is enthalpy of vaporization (or sublimation if $T_s < 273.15$), ΔT is the temperature difference between the atmosphere and the ice surface, Δq is specific humidity difference between the atmosphere and the ice surface, and C_H and C_E are dimensionless bulk transfer coefficients. Strictly speaking, C_H

and C_E depend on atmospheric stability (Launiainen & Cheng, 1998); however, here they are treated as constants approximated based on Parkinson and Washington (1979).

Conductive Heat Flux

Conductive heat flux at the surface of the ice is defined as a temperature gradient between the air and the top layer of the ice:

$$F_i = -k\left(\frac{\partial T}{\partial Z}\right) \tag{9}$$

where T represents the temperature difference defined by the depth Z, and k is the thermal conductivity of the ice. Similarly, heat conduction between ice and the water takes the form of Eq. (9).

Ice ablation and growth

Ice removal from the top of the ice is approximated as a function of net surface radiative heat fluxes, similar to Eq. (3). If the net radiative heat flux (Q_{net}) is greater than zero, the excess energy is used to remove the surface layer of the ice, and can be expressed as:

$$\frac{d_{ABL}}{dt} = -\left(\frac{1}{Lp}\right)\sum Q_{net} \tag{10}$$

where L is latent heat of freezing and p is ice density. Such an approach does not distinguish between sublimation and ice melt; however, it sufficiently represents cumulative annual ice removal from the surface of the ice (Figure 3).

Ice growth is only considered at the bottom of the ice, which is controlled by sensible heat flux from the water, conduction of heat at the ice/water boundary, and latent heat flux associated with the phase change (Danard and others, 1984; Launiainen & Cheng, 1998). The temperature at the ice/water interface is assumed to be at the freezing point. Heat fluxes at the ice/water boundary are difficult to determine because sensible and conductive heat fluxes from the water are difficult to ascertain. Sensible heat from the water can be either approximated as a constant if the water temperature beneath the ice is not known (Launiainen & Cheng, 1998) or calculated, if the water temperature beneath the ice is known, using modified Eq. (7) (Reid and Crout, 2008). However, for proper determination of fluxes from the water column, thermal structure of the water profile should be coupled with the ice (Maykut & Untersteiner, 1971; Launiainen & Cheng, 1998). Here, a second heat equation is solved (Eq. (1)) to calculate the water temperature profile permitting dynamic calculations of heat fluxes between the water and the ice.

Initial Conditions

The initial condition of the ice temperature profile can be approximated as a linear temperature gradient between the ice surface and the ice bottom because the system rapidly adjusts (Reid & Crout, 2008). However, for ice models coupled with ~~the~~ unique water temperature profiles, such as west lobe of Lake Bonney, which takes decades to develop (Vincent and others, 2008), linear approximation might not be appropriate when attempting to model long time series. The initial temperature profiles of the ice and the water column in this model were determined in two steps. First, the temperature gradient between the surface of the ice, ice/water interface, and bottom of the lake was set up as a linear function. The simulation was run until the water temperature profile developed a temperature maximum, similar to that of WLB. Second, the last calculated value, in the previous step, was used as an initial temperature profile for the ice and the water column condition.

Model Validation

The model was validated using 16 ~~years~~ of seasonally measured ice thickness data and 6 ~~years~~ of continuous ablation data from WLB. In addition, modeled vs. measured temperature profiles from WLB are qualitatively compared. The versatility of the model was validated using 16 ~~years~~ of seasonally measured ice thickness data from nearby Lake Fryxell.

The model accurately predicts ice thickness trends for WLB (Figure 4) for the times when ice thickness was measured, including the general trend of increasing ice thickness from 1996 to 2002, followed by the subsequent decrease after 2002. The ice thickness during the measurements in March 2008 when the ice was noted to be flooded with lake water, suggests that the seasonal amplitude of ice thickness variations could be poorly resolved by the model under specific conditions. Despite this deviation, measured vs. modeled ice thickness have a correlation coefficient of $r = 0.95$ ($p < 0.001$) and ~~root-mean-square-error (RMSE)~~ of 0.09 m indicating that the model reasonably captures decadal ice thickness trend variability (Figure 5).

Despite the simplicity of the ablation calculation, cumulative annual ablation is well predicted (Figure 3) with a correlation coefficient of $r = 0.99$ ($p < 0.001$) and RMSE of 0.11 m between measured and modeled ablation. However, the significance of the fit should be interpreted with caution, as r can be artificially inflated with a large number of data points ($n > 4200$). For this reason, RMSE is provided, as it represents an absolute error in units of the data (Willmott, 1981).

The model predicted water temperature profile similar to that of WLB. A typical WLB temperature profile (obtained in 2011) is shown in Figure ~~6A~~ with temperature maximum at ~~approximately~~ 8.5 m depth, which is captured by the modeled temperature maximum (Figure ~~6B~~).

For Lake Fryxell, the model was forced with meteorological data from the Lake Fryxell basin (Figure 1). However, Lake Fryxell ice morphology (and the ice thickness) is significantly different than of WLB and parameters related to optical properties of the ice required adjustment. As such, κ and χ~~,~~ were parameterized (increased) during the simulation. Albedo data for Lake Fryxell ~~is~~ not available and values used for WLB simulations were incorporated. Predicted ice ~~thickness~~ for Lake Fryxell shows a good measured vs. modeled correlation of $r = 0.90$ ($p < 0.001$) and RMSE of 0.21 m (Figure 7).

Model Sensitivity

The model sensitivity was tested by increasing/decreasing variables input by 10% of their nominal value, one at a time. The only exception is air temperature, ~~as 10% change would create unrealistic conditions. Instead, the air temperature~~ sensitivity was tested by an increase/decrease of ~~temperature by~~ 1°K. A simple modified sensitivity index (*Si*) was adapted from Hoffmann and Gardner (1983):

$$Si = \left|1 - \left(\frac{D_{min}}{D_{max}}\right)\right| \quad (11)$$

where D_{min} is model output (ice thickness) when a variable was decreased, and D_{max} is the model output when a variable was increased. Sensitivity index values range from 0 to 1, where 1 represents high sensitivity to a change in a parameter; values ~~less than~~ 0.01 indicate no sensitivity (Hoffmann ~~&~~ Gardner, 1983). Each test was run over a ~~16 year~~ period or until the ice cover melted, whichever came first. The sensitivity test was performed on shortwave radiation (Q_s), air temperature (T_a), bulk transfer coefficients (C_E and C_H), albedo (α), extinction coefficient (κ)~~,~~ and a parameter responsible for partitioning shortwave radiation at the surface of the ice (χ). Sensitivity indices (*Si)* for each parameter are summarized in Table 1, from highest to lowest, and selected parameters are briefly discussed below.

Shortwave radiation is the largest contributor of the energy at the very surface of the ice. As such, the output of the model is highly sensitive to parameters controlling shortwave radiation, including absorption (χ) and reflectance (α) (Table 1). For example, an increase of χ or α decreases solar radiation that penetrates an ice cover, decreasing the overall energy of the system that otherwise would be available for ice melt. This suggests ~~that~~ the model is highly sensitive to parameters controlling surface optical properties of the ice. Q_s and T_a have an inverse effect on the ice cover thickness. An increase of Q_s and T_a significantly contributes to the surface ice temperature, as well as penetrating solar radiation, both of which will enhance melt.

The model is relatively insensitive to changes in bulk transfer coefficients (C_E and C_H~~,~~ respectively). Changes in C_E create small variations in the model's output (yet preserving the long-term trends), whereas~~,~~ changes in C_H make virtually no difference to the output (Table 1). Similar sensitivity results were found by Vincent and others (2008). The sensitivity test validates our original assumption of constant bulk transfer coefficients, reducing the computational complexity of the model.

Lake ice thickness is controlled by the surface energy balance and is presumed to reflect climatic changes (Wharton and others, 1992~~;~~ Reid ~~&~~ Crout, 2008). Taylor Valley experienced a general cooling trend between 1986 and 1999 (0.7 ~~°C per decade~~), associated with increasing lake ice thickness (0.11 m a^{-1}) and increasing shortwave radiation (8.1 W m^{-2} ~~per decade~~), based on meteorological data from the Lake Hoare basin (Doran and others, 2002b). Since early- to mid-2000, the increasing ice-thickness trends reversed: WLB ice thickness started to decrease in 2002 (Fig~~ure~~ 4) whereas the ice thickness of Lake Fryxell started to decline in 2006 (Fig~~ure~~ 7). The most notable change in the Taylor Valley climate during this time period was an exceptionally warm summer season during 2001/2002 when maximum air temperature was ~~greater than~~ 9 °C (Doran and others, 2008~~;~~ Barrett and others, 2008).

The influence of seasonal temperature extremes on the long-term ice thickness trends is explored below. A sensitivity experiment was designed where the exceptionally warm season meteorological data of 2001/2002 were substituted with meteorological data from an unusually cold season from the year prior (for WLB). The simulation results show no changes in the ice

thickness trend ($r = 0.98$, $p < 0.001$). Conversely, the unusually cold season meteorological data, from a previous year, were randomly forced in the model during the ice thickness decline to test whether it would influence the long-term ice thickness trends. No changes in the trends were detected following this forcing, indicating that the long-term ice thickness trends in Taylor Valley lakes are not particularly responsive to discrete warming/cooling events. Rather, water column heat flux plays a major role in regulating ice thickness of the study lakes.

Discussion

Predictions of long-term ice thickness trends of stratified perennially ice-covered lakes must consider the unique temperature profile of the water column of a lake as an additional heat source. In Antarctica's perennially ice-covered lakes, heat accumulates in the water column due to the continuous influx of solar radiation during austral summers (Chinn, 1993; Shirtcliffe & Benseman, 1964). The deep water temperature maximum associated with higher salt content takes decades to develop (Vincent and others, 2008).

Thermal structures of water columns can influence long-term ice thickness trends and preclude a response of the ice thickness to climatic changes. The water column temperature in Taylor Valley lakes is controlled by penetrating solar radiation (Shirtcliffe & Benseman, 1964; Vincent and others, 2008; Spigel & Priscu, 1998). Penetrating solar radiation decays with depth in the ice and the water column based on the extinction coefficients. As a result, shallow water receives more energy than deep water and it will be more responsive to seasonal variations of penetrating solar radiation. Additionally, shallow water temperature is influenced by the contribution of sensible heat flux from the seasonal stream input, which enhances ice thinning. However, it is not included in the model. The energy stored at depth (long-term storage) will affect shallow water temperature, to a certain extent, by the upward heat conduction due to the thermal gradient. As a conceptual example, for a deep lake with a temperature maximum at some depth, during a climate cooling trend (assuming constant shortwave radiation), shallow waters will cool ~~down~~, increasing ice growth rates. Yet, shallow water will cool at rates slower than that of the air due to an influx of heat from the deep lake heat storage. The incoming heat from beneath will hinder shallow water cooling and slow ice thickness growth (~~example,~~ Figure 8). Conversely, for shallow lakes that do not have a deep temperature maximum, this process will be less pronounced and the shallow water temperature will more closely reflect climate cooling (Figure 9). The situation would reverse during climate warming; the ice thickness of deep lakes with a well-developed temperature maximum would respond to surface air warming quicker due to the additional heat flux from beneath. For example, the ice thickness of WLB responded earlier to the increase of surface air ~~temperatures (Figures 4 and 8)~~ between 2000 and 2012 in comparison with ice thickness of Lake Fryxell ~~(Figures 7 and 9)~~. This suggests that lakes with deep temperature maxima can reduce the response of ice thickness to climatic changes.

The modeled water temperature profile of WLB shows three distinct trends: a continuous increase of deep water temperature over time, a continuous decrease of temperature maximum within about the first 5 ~~meters~~ under the ice cover (Figure 6), and a shallow water temperature (immediately beneath the ice) that varies inversely with the ice thickness ($r = -0.85$, $p < 0.001$) (Figure 8). Annually measured temperature profiles of WLB show similar trends (unpublis data). The only exception in measured data is an increase of temperature maximum after 2009, which is not captured by the model. The cooling of shallow water is associated with an ice thickness increase from 1996 to the end of 2001 (Figure 8). Conversely, the warming of shallow water is associated with an ice thickness decrease after 2001 (Figure 8). A similar trend of

inversely proportional ice thickness and shallow water temperature is observed at Lake Fryxell; however, a clear temporal change in ice thickness and water temperature occurred in 2005 (Figure 9). The difference in response time of the ice thickness in these two lakes can be attributed to the different thermal structures of the water columns near the ice-water interface, which is influenced by the deep thermal heat storage.

The observed long-term ice thickness trends in both lakes are a result, first and foremost, of the thermal structure of the water column and surface energy balance. The infrequent seasonal temperature warming do not influence long-term ice thickness trends because a secondary process (heat flux from the water column) that is driven on much longer timescale influences the long-term trends of ice thickness. The alteration of the ice thickness trend occurs at a threshold dictated by heat fluxes at the ice surface and shallow water temperature, which is influenced by the thermal structure of the water column. Shallow water temperature is controlled by the penetrating shortwave radiation and the heat flux from deep waters. As a result, lake ice thickness will respond to climate forcings on different time scales depending on the thermal structure of the lake in question. We suggest that shallow perennially ice-covered lakes, such as Lake Fryxell, are a better proxy for climate change, owing to the fact that the ice thickness response to long-term climate forcing is not affected by the deep thermal water maximum.

Conclusions

A thermodynamic model parameterized for ice cover of WLB was developed. The model is driven by surface radiative heat fluxes and heat fluxes from the underlying water column, coupled with two one-dimensional heat equations. The water temperature profile is calculated in order to properly constrain heat fluxes at the ice/water boundary. Despite the simplistic nature of the model (it does not account for physics associated with isothermal ice, advection of the water column, and sensible heat associated with stream inflow), the model successfully calculates long-term ice thickness changes as well as the temperature profile of the ice and the water column in two stratified lakes. Predicted ice thickness changes are in good agreement with trends observed in measured ice thickness data.

Perennially ice-covered lakes with a deep-water temperature maximum will impede the response of ice thickness growth to surface air-cooling. The impact of surface air-cooling is hindered by the heat flux from the water column. Conversely, during surface air warming, the water temperature maximum facilitates ice decay, due to an additional heat flux from below. Ice thickness of shallow lakes (<20 m), on the other hand, will more accurately respond to climatic changes because of diminished effect of the water column temperature on the ice thickness. Hence, ice covers can be used as indicators of climate change; however, the ice thickness trends should be interpreted with caution due to the influence of thermal stratification of the water column.

Acknowledgments

This research was supported by the Office of Polar Programs (grants 9810219, 0096250, 0832755, 1041742, and 1115245). Logistical support was provided by the US Antarctic Program through funding from NSF. We thank the Long Term Ecological Research project personnel for collecting the ice thickness measurements throughout the duration of this project and Douglas MacAyeal for insightful conversations on the topic.

Adams, E.E., J. Priscu, C.H. Fritsen, S.R. Smith and S.L. Brackman 1998. Permanent ice covers of the McMurdo Dry Valley lakes, Antarctica: bubble formation and metamorphism. In Priscu, J.C., *ed. Ecosystem dynamics in a polar desert; the McMurdo dry valleys, Antarctica.*, American Geophysical Union, 281-295. (Antarctic Research Series.

Andersen, D.T., C.P. McKay and R.A. Wharton 1998. Dissolved gases in perennially ice-covered lakes of the McMurdo dry valleys, Antarctica. *Antarctic Science*, **10**(2): 124-133.

Barrett, J.E., R.A. Virginia, D.H. Wall, P.T. Doran, A.G. Fountain, K.A. Welch and W.B. Lyons 2008. Persistent effects of a discrete warming event on a polar desert ecosystem. *Global Change Biology*, **14**(10): 2249-2261.

Bennett, T.J. 1982. A Coupled Atmosphere-Sea Ice Model Study of the Role of Sea Ice in Climatic Predictability. *Journal of the Atmospheric Sciences*, **39**(7): 1456-1465.

Bintanja, R. and M.R. Vandenbroeke 1995. The Surface-Energy Balance of Antarctic Snow and Blue Ice. *Journal of Applied Meteorology*, **34**(4): 902-926.

Brandt, R.E. and S.G. Warren 1993. Solar-Heating Rates and Temperature Profiles in Antarctic Snow and Ice. *Journal of Glaciology*, **39**(131): 99-110.

Chinn, T.J. 1993. Physical hydrology of the dry valley lakes. In Green, W.J. and E.I. Friedmann, *eds. Physical and Biogeochemical Processes in Antarctic Lakes*, American Geophysical Union, 1-51. (Antarctic Research Series.

Danard, M., M. Gray and G. Lyv 1984. A Model for Predicting Ice Accretion and Ablation in Water Bodies. *Monthly Weather Review*, **112**(6): 1160-1169.

Doran, P.T., G.L. Dana, J.T. Hastings and R.A.J. Wharton 1995. McMurdo Dry Valleys Long-Term Ecological Research (LTER): LTER automatic weather network (LAWN). *Antarctic Journal of the U.S.*, **30**(5): 276-280.

Doran, P.T., C.P. McKay, G.D. Clow, G.L. Dana, A. Fountain, T. Nylen and W.B. Lyons 2002a. Valley floor climate observations from the McMurdo Dry Valleys, Antarctica, 1986-2000. *Journal of Geophysical Research*, **107 (D24)**: 4772, doi:10.1029/2001JD002045.

Doran, P.T., C.P. McKay, A.G. Fountain, T. Nylen, D.M. McKnight, C. Jaros and J.E. Barrett 2008. Hydrologic response to extreme warm and cold summers in the McMurdo Dry Valleys, East Antarctica. *Antarctic Science*, **20**(5): 499-509.

Doran, P.T., J.C. Priscu, W.B. Lyons, J.E. Walsh, A.G. Fountain, D.M. McKnight, D.L. Moorhead, R.A. Virginia, D.H. Wall, G.D. Clow, C.H. Fritsen, C.P. McKay and A.N. Parsons 2002b. Antarctic climate cooling and terrestrial ecosystem response. *Nature*, **415**(6871): 517-520.

Doran, P.T., R.A. Wharton, Jr. and W.B. Lyons 1994. Paleolimnology of the McMurdo Dry Valleys, Antarctica. *Journal of Paleolimnology*, **10**(2): 85-114.

Dugan, H.D., M.K. Obryk and P.T. Doran 2013. Lake ice ablation rates from permanently ice-covered Antarctic lakes. *Journal of Glaciology*, **59**(215): 491-498.

Fountain, A., W.B. Lyons, M.B. Burkins, G.L. Dana, P.T. Doran, K.J. Lewis, D. McKnight, D.L. Moorhead, A.N. Parsons, J.C. Priscu, D.H. Wall, R.A.J. Wharton and R.A. Virginia 1999. Physical controls on the Taylor Valley Ecosystem, Antarctica. *Bioscience*, **49**(12): 961-972.

Fritsen, C.H. and J.C. Priscu 1999. Seasonal change in the optical properties of the permanent ice cover on Lake Bonney, Antarctica: consequences for lake productivity and phytoplankton dynamics. *Limnology and Oceanography*, **44**(2): 447-454.

Guest, P.S. 1998. Surface longwave radiation conditions in the eastern Weddell Sea during winter. *Journal of Geophysical Research-Oceans*, **103**(C13): 30761-30771.

Gupta, S.C. 2003. *The classical Stefan problem : basic concepts, modelling, and analysis.* Amsterdam ; Boston, Elsevier.

Hoffmann, F.O. and R.H. Gardner 1983. Evaluation of uncertainties in environmental radiological assessment models. US Nuclear Regulatory Commission NUREG/CR-3332.

Konig-Langlo, G. and E. Augstein 1994. Parameterization of the downward long-wave radiation at the Earth's surface in polar regions. *Meteorol. Zeitschrift*, **3**: 343-347.

Launiainen, J. and B. Cheng 1998. Modelling of ice thermodynamics in natural water bodies. *Cold Regions Science and Technology*, **27**(3): 153-178.

Liston, G.E., J. Winther, O. Brunland, H. Elvehoy and K. Sand 1999. Below-surface ice melt on the coastal Antarctica ice sheet. *Journal of Glaciology*, **45**(150): 273-284.

Lumb, F.E. 1964. The influence of cloud on hourly amounts of total radiation on the sea surface. *Quart. J. R. Met. Soc.*, **90**: 43-56.

Maykut, G.A. and N. Untersteiner 1971. Some Results from a Time-Dependent Thermodynamic Model of Sea Ice. *Journal of Geophysical Research*, **76**(6): 1550-&.

McKay, C.P., G.D. Clow, D.T. Andersen and R.A. Wharton 1994. Light transmission and reflection in perennially ice-covered Lake Hoare, Antarctica. *Journal of Geophysical Research*, **99**(C10): 20427-20444.

McKay, C.P., G.D. Clow, R.A. Wharton and S.W. Squyres 1985. Thickness of ice on perennially frozen lakes. *Nature*, **313**(6003): 561-562.

Parkinson, C.L. and W.M. Washington 1979. Large-Scale Numerical-Model of Sea Ice. *Journal of Geophysical Research-Oceans and Atmospheres*, **84**(Nc1): 311-337.

Priscu, J.C., M.T. Downes and C.P. McKay 1996. Extreme supersaturation of nitrous oxide in a poorly ventilated Antarctic lake. *Limnology and Oceanography*, **41**(7): 1544-1551.

Reid, T. and N. Crout 2008. A thermodynamic model of freshwater Antarctic lake ice. *Ecological Modelling*, **210**(3): 231-241.

Scott, R.F. 1905. *The Voyage of Discovery.* London, McMillan and Co.

Shirtcliffe, T.G.L. and R.F. Benseman 1964. A sun-heated Antarctic lake. *J. Geophys. Res.*, **69** 3355-3359.

Spigel, R.H. and J.C. Priscu 1996. Evolution of temperature and salt structure of Lake Bonney, a chemically stratified Antarctic lake. *Hydrobiologia*, **321**(3): 177-190.

Spigel, R.H. and J.C. Priscu 1998. Physical limnology of the McMurdo Dry Valley lakes. In Priscu, J.C., *ed. Ecosystem Dynamics in a Polar Desert: The McMurdo Dry Valleys, Antarctica*, Washington, D.C., American Geophysical Union, 153-187.

Trefethen, L.N. 2000. *Spectral methods in MATLAB.* Philadelphia, Pa., Society for Industrial and Applied Mathematics.

Vincent, A.C., D.R. Mueller and W.F. Vincent 2008. Simulated heat storage in a perennially ice-covered high Arctic lake: Sensitivity to climate change. *Journal of Geophysical Research*, **113**(C4).

Wharton, R.A., C.P. McKay, G.D. Clow, D.T. Andersen, G.M. Simmons and F.G. Love 1992. Changes in Ice Cover Thickness and Lake Level of Lake Hoare, Antarctica - Implications for Local Climatic-Change. *Journal of Geophysical Research*, **97**(C3): 3503-3513.

Wharton, R.A., C.P. McKay, G.M. Simmons and B.C. Parker 1986. Oxygen Budget of a Perennially Ice-Covered Antarctic Lake. *Limnology and Oceanography*, **31**(2): 437-443.

Wharton, R.A., G.M. Simmons and C.P. McKay 1989. Perennially Ice-Covered Lake Hoare, Antarctica - Physical-Environment, Biology and Sedimentation. *Hydrobiologia*, **172**: 305-320.

Willmott, C.J. 1981. On the validation of models. *Physical Geography*, **2**(2): 184-194.

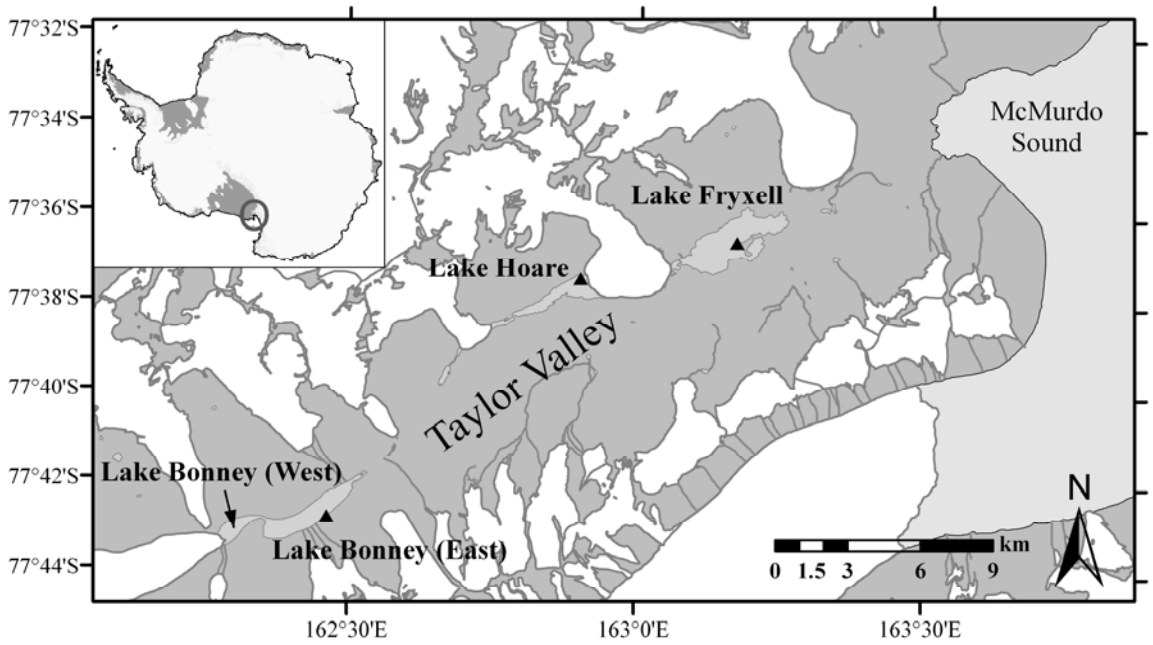

Figure 1. Map of Taylor Valley, Antarctica. Triangles indicate locations of meteorological stations.

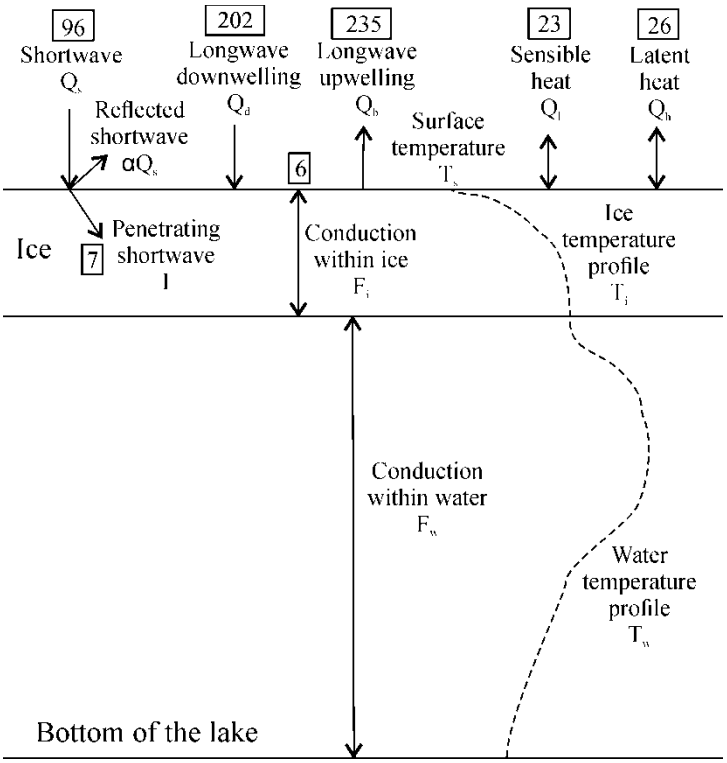

Figure 2. Conceptual representation of heat fluxes and temperature profile for west lobe of Lake Bonney. Numbers in boxes represent annually averaged fluxes (W m^{-2}).

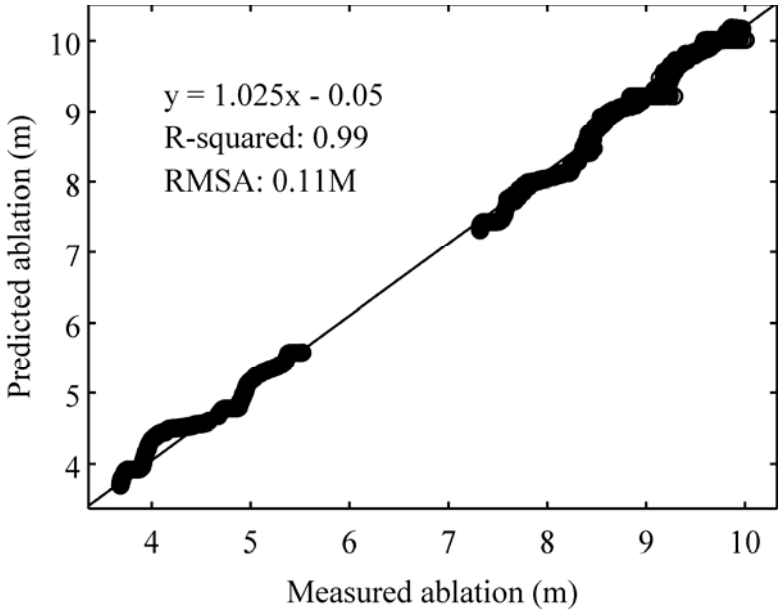

Figure 3. Linear fit between 6 ~~years~~ of overlapping measured and predicted ice ablation for west lobe of Lake Bonney (each data point represent 12-hr averages, n = 4251). ~~RMSE is Root-Mean-Square-Error.~~

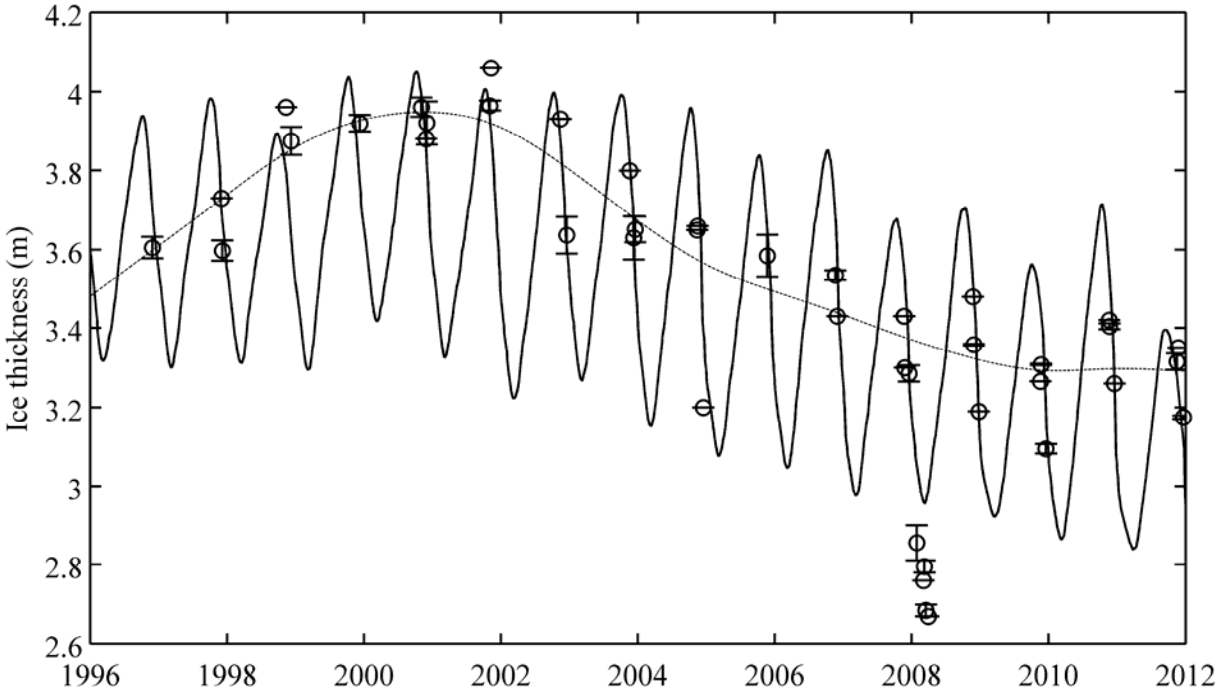

Figure 4. Predicted ice thickness changes for west lobe of Lake Bonney (black solid ~~line~~) and averaged measured ice thickness (circles) from 1996 to 2012. Numerous ice thickness measurements were obtained during the same day, showing large variability. Days with multiple ice thickness measurements were averaged. Error bars are shown as standard deviation. Dashed ~~line~~ represents a spline fit to measured data, excluding late season 2008 measurements.

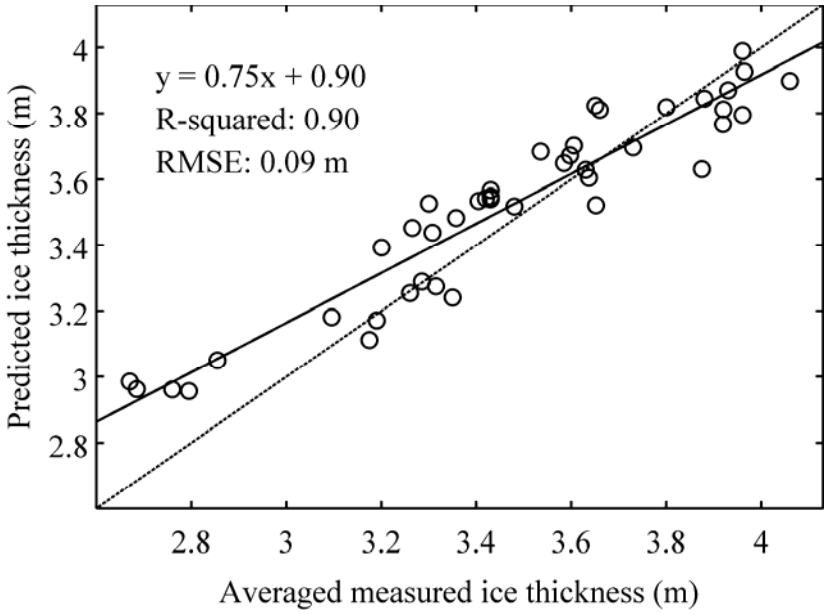

Figure 5. Linear fit between 16 ~~years~~ of overlapping measured and predicted ice thickness changes for west lobe of Lake Bonney. Circles represent daily averaged overlapping data. ~~RMSE is Root-Mean-Square-Error.~~ Dashed line is 1:1.

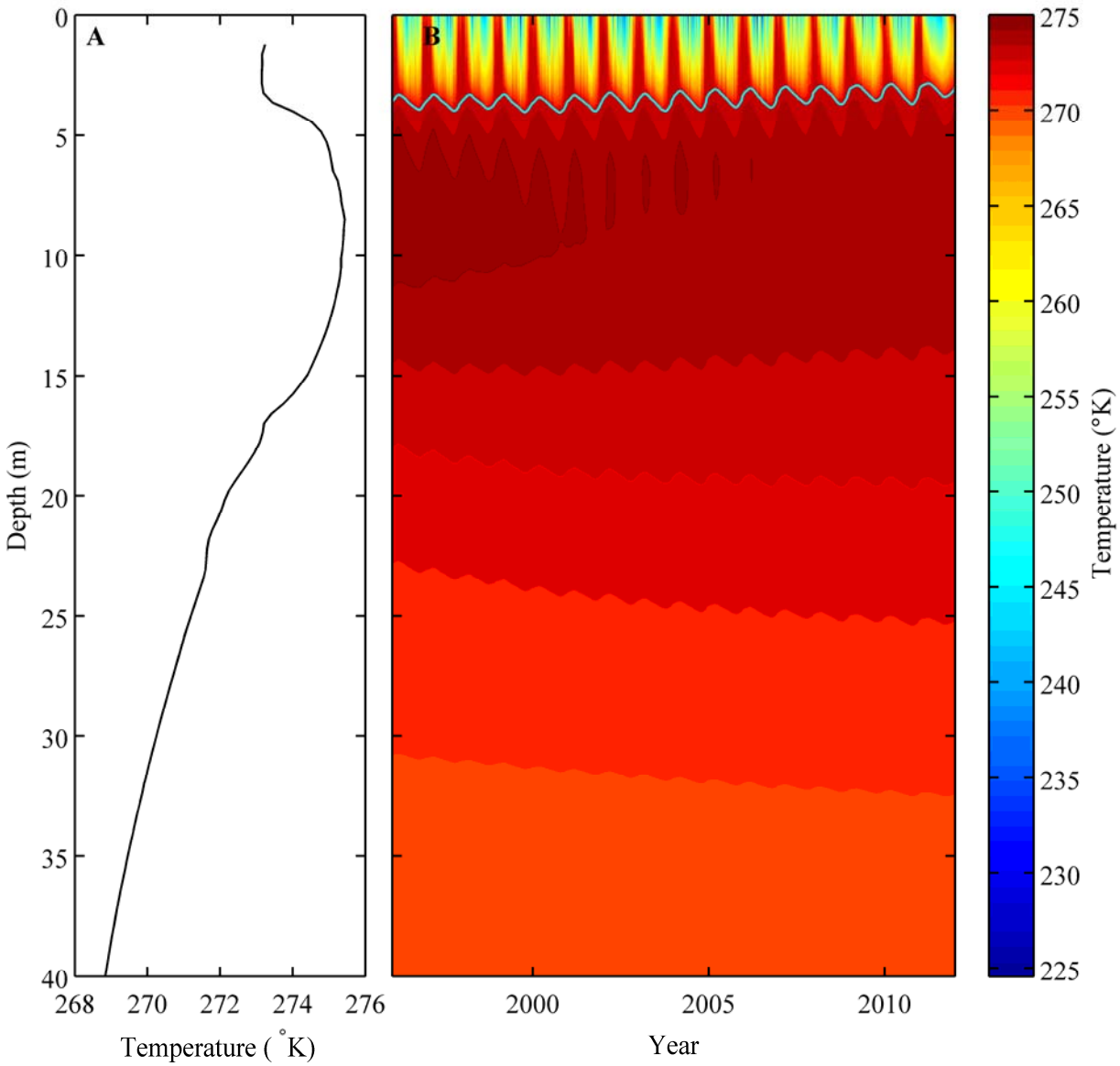

Figure 6. ~~A)~~ A typical water temperature profile from west lobe of Lake Bonney (data obtained ~~on Nov 21st 2011).~~ B) Modeled evolution of water temperature profile between 1996 and 2012.

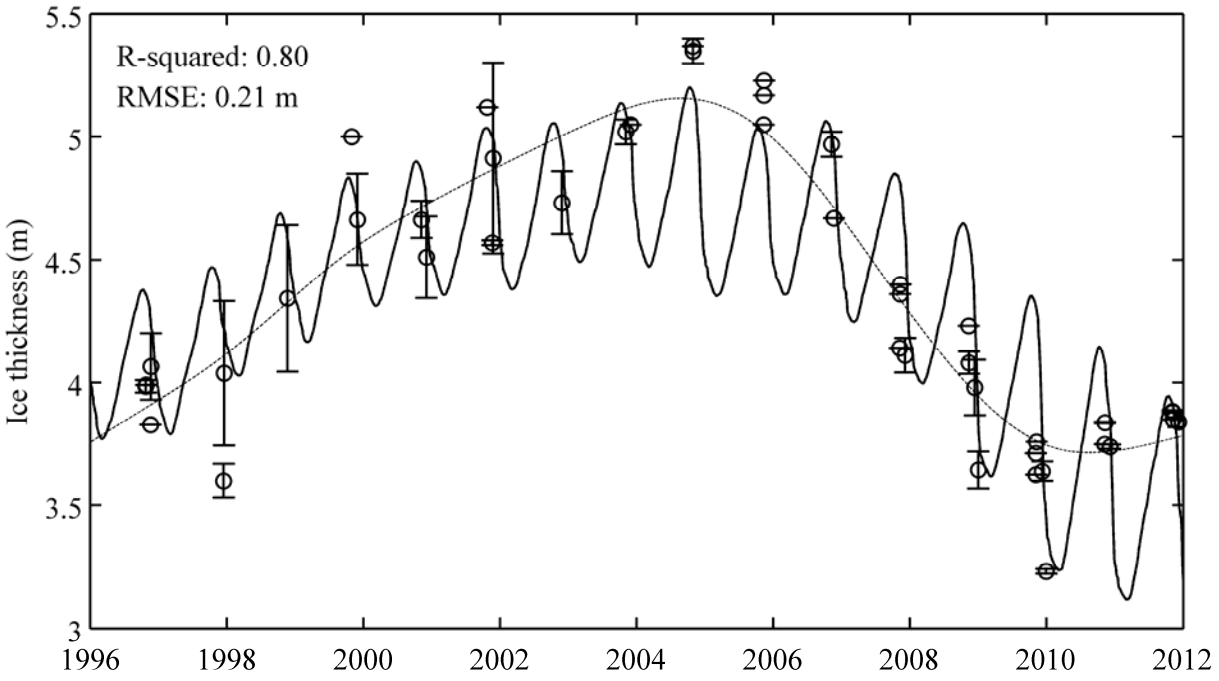

Figure 7. Predicted ice thickness changes for Lake Fryxell (solid ~~line~~) and averaged measured ice thickness (circles) from 1996 to 2012. Numerous ice thickness measurements were obtained during the same day, showing large variability. Days with multiple ice thickness measurements were averaged. Error bars are shown as standard deviation. ~~RMSE – Root-Mean-Square-Error.~~ Dashed ~~line~~ represents a spline fit to measured data, excluding late season 2008 measurements.

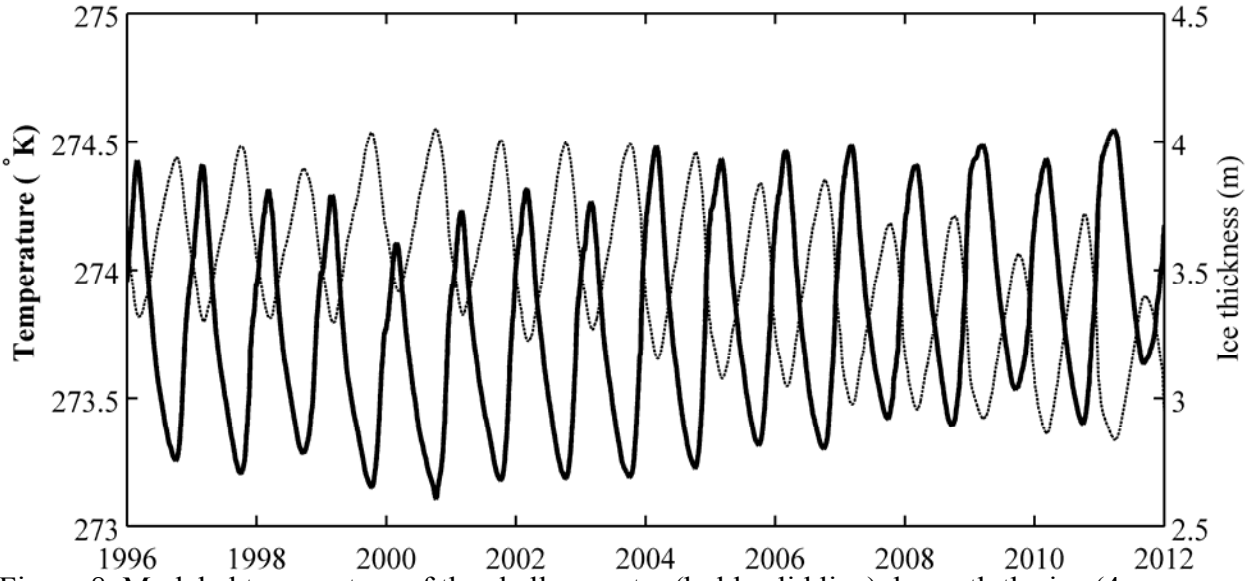

Figure 8. Modeled temperature of the shallow water (bold solid ~~line~~), beneath the ice (4 m depth), over time at west lobe of Lake Bonney and modeled ice thickness change over time (dashed ~~line~~). Shallow water temperature and ice thickness changes are inversely proportional.

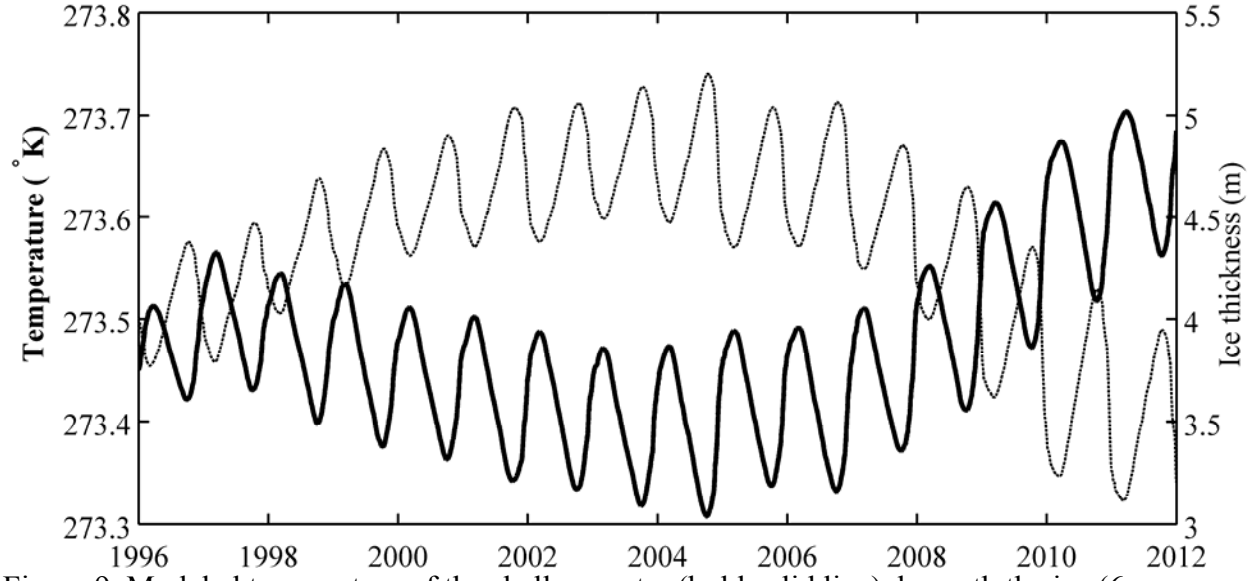

Figure 9. Modeled temperature of the shallow water (bold solid ~~line~~), beneath the ice (6 m depth), over time at Lake Fryxell and modeled ice thickness change over time (dashed ~~line~~). Shallow water temperature and ice thickness changes are inversely proportional.

Table 1. Sensitivity Index (*Si*) results for parameters used in the model. Values ~~less than~~ 0.01 represent no sensitivity to the changes, whereas *Si* of 1 indicates large sensitivity ~~the~~ changes. χ – wavelength depended absorption of shortwave radiation at the surface of the ice, α – albedo, Q_s – shortwave radiation, T_a – air temperature, C_E – bulk transfer coefficient used in latent heat equation, C_H – bulk transfer coefficient used in the sensible heat equation, κ – extinction coefficient.

	χ	α	Q_s	T_a	C_E	C_H	κ
Si	0.46	0.33	0.27	0.19	0.06	< 0.01	< 0.01